Achievable Rate with 1-Bit Quantization and Oversampling at the Receiver using Continuous Phase Modulation

Lukas T. N. Landau*, Meik Dörpinghaus†, Rodrigo C. de Lamare*, and Gerhard P. Fettweis†
*Centro de Estudos em Telecomunicações, Pontifícia Universidade Católica do Rio de Janeiro
Rio de Janeiro CEP 22453-900, Brazil, Email: {landau, delamare}@cetuc.puc-rio.br
†Vodafone Chair Mobile Communications Systems, SFB 912 HAEC, Technische Universität Dresden
01062 Dresden, Germany, Email: {meik.doerpinghaus, gerhard.fettweis}@tu-dresden.de

***Abstract*—Analog-to-digital conversion with high resolution in amplitude has a relatively high energy consumption in communication systems. A promising alternative is 1-bit quantization and oversampling at the receiver. We consider continuous phase modulation which is favorable because of its bandwidth efficiency and its constant envelope. Because the information is conveyed in the phase transitions of these signals, oversampling is a promising strategy for detection. The additional degrees of freedom brought by oversampling at the receiver can be exploited by a higher-order modulation. A lower bound on the achievable rate is computed based on an auxiliary channel law. Our computational results show that oversampling increases the achievable rate in general. The proposed approach enables a 90% power containment bandwidth efficiency slightly lower than existing methods with 1-bit quantization and oversampling while gaining the advantages of the constant envelope modulation.**

***Index Terms*—Quantization, 1-bit, oversampling, ADC, continuous phase modulation, achievable rate, low-IF.**

I. Introduction

Coarse quantization at the receiver is favorable in terms of energy efficiency, which is a fundamental matter for high sampling rates as required by multigigabit/s communication. In the present study, a special case is considered where the receiver has only sign information about the received signal. Oversampling with respect to the temporal duration of a transmit symbol is used to compensate for the loss in terms of the achievable rate. This setup is considered in combination with continuous phase modulation (CPM), which is known to be bandwidth efficient, having smooth phase transitions and a constant envelope [1], [2]. The advantage of having a constant envelope allows for energy efficient power amplifiers with limited dynamic range. The information is implicitly conveyed in phase transitions, which makes the consideration of additional samples between the phase states promising in the presence of coarse quantization at the receiver. This property has been exploited already in [3], where the output signal of an integrate-and-dump receiver is sampled with oversampling rate instead of a bank of matched filters. In contrast to the work in [3] we devise an even simpler receiver, which relies on 1-bit quantization and we consider also higher-order modulation schemes.

Initially, a marginal benefit of 1-bit quantization and oversampling at the receiver in terms of the achievable rate has been reported in [4], where a bandlimited channel is considered. Soon after, in [5] a significant benefit of 1-bit quantization and oversampling a Zakai bandlimited process [6] has been shown. In both studies [4], [5] a noiseless channel is considered. However, by considering the capacity per unit cost, it has been shown in [7] that 1-bit quantization and oversampling at the receiver can also be beneficial in a noisy scenario. More recently, the high signal-to-noise ratio (SNR) regime has been considered based on the concept of the generalized mutual information [8], which results in a minor benefit in terms of achievable rate for oversampling ratios larger or equal to 4. More promising is the novel approach presented in [9], where the achievable rate of the bandlimited channel is lower-bounded by a truncation based auxiliary channel law. The resulting channel has a finite state memory, where a sequence design is beneficial in terms of achievable rate. By the consideration of sequences, described by optimized Markov sources, a significant gain in term of achievable rate is observed in [9] when oversampling the channel output signal.

In addition, there are a number of studies on channels with less strict bandwidth constraints. In what follows, all those approaches are briefly specified. In this regard, a memoryless channel with rectangular shaped waveform has been discussed in [10]. In [11] the intersymbol interference caused by Bessel filters at the transmitter and the receiver is exploited in the sense of a random dithering signal. A sequence design strategy for the design of reconstructible 4-ASK modulated sequences is reported in [12]. Recently, in [13] a sequence design for faster-than-Nyquist signaling has been suggested. Later the approach has been extended by a filter optimization with regard to a given spectral mask [14] suitable for 60 GHz communication channels. Another study has considered a waveform design, which allows the transmission of independent identically distributed (i.i.d.) 16-QAM symbols [15]. The corresponding approaches for massive MISO and MIMO channels have been studied in [16] and [17], respectively.

In this work we consider the design an analysis of CPM

schemes with 1-bit quantization and oversampling at the receiver. Most of the above mentioned approaches on 1-bit quantization and oversampling refer especially to energy efficient receivers. In a number of cases this comes at a price of increased complexity at the transmitter, e.g., increased number of transmit antennas [16] or at least increased peak-to-average power ratio (PAPR) [12]–[15] in comparison to a QPSK modulation with Nyquist rate signaling which thus does not allow for the utilization for highly efficient power amplifiers. Different to our previous studies on communications with 1-bit quantization and oversampling at the receiver, e.g., [12]–[14], in this work we propose to use CPM as the modulation format, which has the advantage of a constant envelope and with this it yields a low PAPR. For numerical evaluation of the achievable rates we consider a bandpass receive filter, which is similar to the integrate-and-dump receiver proposed in [3]. The corresponding discrete-time channel consisting of the CPM modulator, additive white Gaussian noise and receive filter, has memory. Our main contributions are the introduction of a system model for CPM signals received with 1-bit quantization and oversampling and the derivation of a lower bound on the achievable rates by using an auxiliary channel law.

The rest of the paper is organized as follows. In Section II, the system model of CPM is given, followed by the description of the time invariant trellis. Section II concludes with the proposed discrete system model, taking into account 1-bit quantization and oversampling at the receiver. The computation of the lower bound on the achievable rate is discussed in Section III which implies the introduction of the auxiliary channel law. The numerical results are presented in Section IV where the benefits of oversampling and higher-order modulation are evaluated and a conclusion is given in Section V.

Notation: To express probabilities of random quantities we use the simplified notation with $P(\boldsymbol{y}^n|x^n) = P(\boldsymbol{Y}^n = \boldsymbol{y}^n|X^n = x^n)$, where the random quantities are denoted by capital letters and its realizations by lower-case letters. Bold symbols denote vectors, namely oversampling vectors, e.g., $\boldsymbol{y}_k$ is a column vector with M entries, where k indicates the kth symbol in time or rather its corresponding time interval. Sequences are denoted with $x^n = [x_1, \ldots, x_n]^T$. Likewise, sequences of vectors are written as $\boldsymbol{y}^n = [\boldsymbol{y}_1^T, \ldots, \boldsymbol{y}_n^T]^T$. A segment of a sequence is given by $x_{k-L}^k = [x_{k-L}, \ldots, x_k]^T$ and $\boldsymbol{y}_{k-L}^k = [\boldsymbol{y}_{k-L}^T, \ldots, \boldsymbol{y}_k^T]^T$.

II. System Model

The CPM signal in the passband with carrier frequency f_0 [1] is described by

$$s(t) = \mathrm{Re}\left\{\sqrt{\frac{2E_\mathrm{s}}{T_\mathrm{s}}}e^{j(2\pi f_0 t+\phi(t))}\right\}, \tag{1}$$

where $\mathrm{Re}\{\cdot\}$ denotes the real part. The phase term is given by

$$\phi(t) = 2\pi h\sum_{k=0}^{\infty}\alpha_k f(t-kT_\mathrm{s}) + \varphi_0, \tag{2}$$

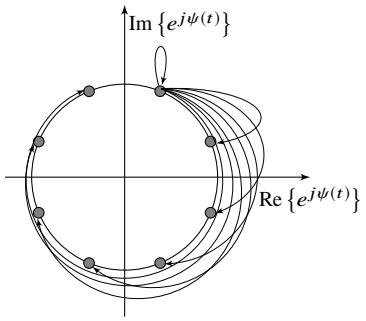

Fig. 1. Constellation diagram of the tilted continuous phase modulation

where T_s denotes the symbol duration, $h = \frac{K_\mathrm{cpm}}{P_\mathrm{cpm}}$, $f(\cdot)$ is the phase response, φ_0 is a phase-offset and α_k represents the transmit symbols with symbol energy E_s. In order to obtain a finite number of phase states K_cpm and P_cpm are relatively prime positive integers. It is considered that the phase response function fulfills the condition

$$f(\tau) = \begin{cases} 0, & \text{if } \tau \le 0, \\ \frac{1}{2}, & \text{if } \tau > L_\mathrm{cpm}T_\mathrm{s}, \end{cases}$$

where L_cpm describes the depth of the memory in terms of transmit symbols. The phase response corresponds to the integration over the frequency pulse $g_f(\cdot)$, which is conventionally a rectangular pulse, a truncated and raised cosine pulse, or a Gaussian pulse. The transmit symbols are drawn from an alphabet described by

$$\alpha_k \in \begin{cases} \{\pm 1, \pm 3, \ldots, \pm(M_\mathrm{cpm}-1)\}, & \text{if } M_\mathrm{cpm} \text{ even}, \\ \{0, \pm 2, \pm 4, \ldots, \pm(M_\mathrm{cpm}-1)\}, & \text{if } M_\mathrm{cpm} \text{ odd}, \end{cases}$$

with M_cpm as the input cardinality.

1) Tilted Time Invariant Trellis: Referring to (2) the corresponding trellis is in general time variant, which means that the possible phase states are time-dependent. With this, the number of states can be larger than M_cpm, e.g., when $M_\mathrm{cpm} = 2$ and $h = \frac{1}{2}$, there are at least four trellis states in total and even more depending on the memory of the channel. In order to reduce the complexity at the receiver, a time invariant trellis is constructed by tilting the trellis according to the decomposition approach in [18]. As a result, the trellis is constructed such that the constellation diagram with its phase states and transitions can be described by Fig. 1. In this work the constellation diagram is of special interest because the zero-crossings can be highlighted easily. A zero-crossing of the CPM signal occurs whenever the transition of the phase corresponds to a crossing of the real or imaginary axis. The tilt corresponds to an extension of the phase term given by (2) as

$$\psi(t) = \phi(t) + \pi h\left(M_\mathrm{cpm}-1\right)\frac{t}{T_\mathrm{s}}, \tag{3}$$

where the 2nd term on the RHS corresponds to the tilt of the trellis. Taking the derivative of the tilt with respect to time and

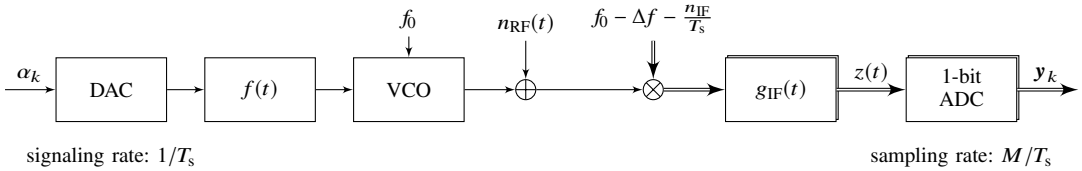

Fig. 2. System model, continuous phase modulation sampled at a low-IF, with 1-bit quantization and oversampling at the receiver

dividing by 2π results in a frequency offset with

$$\Delta f = \frac{h(M_{\mathrm{cpm}} - 1)}{2T_{\mathrm{s}}}. \tag{4}$$

Substituting the symbol notation by $x_k = (\alpha_k + M_{\mathrm{cpm}} - 1)/2$ corresponds to the symbol alphabet $x_k \in \{0, 1, \ldots, M_{\mathrm{cpm}} - 1\}$. According to [18] the phase expression within one symbol duration is denoted with x_k as

$$\begin{aligned}\psi(\tau + kT_{\mathrm{s}}) =& 2\pi h \sum_{l=0}^{k-L_{\mathrm{cpm}}} x_l + 4\pi h \sum_{l=0}^{L_{\mathrm{cpm}}-1} x_{k-l} f(\tau + lT_{\mathrm{s}}) \\ &+ \pi h (M_{\mathrm{cpm}} - 1)\frac{\tau}{T_{\mathrm{s}}} \\ &- 2\pi h \left(M_{\mathrm{cpm}} - 1\right) \sum_{l=0}^{L_{\mathrm{cpm}}-1} f(\tau + lT_{\mathrm{s}}) \\ &+ \left(L_{\mathrm{cpm}} - 1\right)\left(M_{\mathrm{cpm}} - 1\right)\pi h + \varphi_0 \quad , 0 \le \tau < T_{\mathrm{s}}.\end{aligned} \tag{5}$$

Applying the $\bmod 2\pi$ operator to the first term on the right hand side of (5) yields

$$\begin{aligned}\left(2\pi h \sum_{l=0}^{k-L_{\mathrm{cpm}}} x_l\right) \bmod 2\pi &= \frac{2\pi}{P_{\mathrm{cpm}}}\left(\left(K_{\mathrm{cpm}} \sum_{l=0}^{k-L_{\mathrm{cpm}}} x_l\right) \bmod P_{\mathrm{cpm}}\right) \\ &= \frac{2\pi}{P_{\mathrm{cpm}}}\beta_{k-L_{\mathrm{cpm}}},\end{aligned} \tag{6}$$

which introduces the absolute phase state β_k. With this, the phase expression for one symbol duration can be fully described by the absolute phase state $\beta_{k-L_{\mathrm{cpm}}}$ and the previous and the current transmit symbols $x_{k-L_{\mathrm{cpm}}+1}^{k}$ given by $\tilde{s}_k = \left[\beta_{k-L_{\mathrm{cpm}}}, x_{k-L_{\mathrm{cpm}}+1}^{k}\right]$. We want to highlight, that $\tilde{s}_k$ is the appropriate state description for the modeling of the signal at the intermediate frequency. To model the signal which has passed the bandpass filter at the intermediate frequency another state description, namely s_k will be introduced. We set $\varphi_0 = \pi h$ instead of $\varphi_0 = 0$ whenever it avoids phase states placed on the axis in the constellation diagram, which is the case in all the considered examples.

2) Receiving at Low-IF: The tilted trellis corresponds to a frequency offset (4) which can be understood as an intermediate frequency (IF). Furthermore, a suitable time-invariant trellis is preserved when considering a low-IF, such that the the corresponding phase term is given by

$$\psi_{\mathrm{IF}}(\tau + kT_{\mathrm{s}}) = \psi(\tau + kT_{\mathrm{s}}) + 2\pi\frac{n_{\mathrm{IF}}}{T_{\mathrm{s}}}\tau, \tag{7}$$

where n_{IF} is an arbitrary non-negative integer. With this, valid intermediate frequencies are given by

$$\left(\Delta f + \frac{n_{\mathrm{IF}}}{T_{\mathrm{s}}}\right) = \frac{h(M_{\mathrm{cpm}} - 1)}{2T_{\mathrm{s}}} + \frac{n_{\mathrm{IF}}}{T_{\mathrm{s}}}, \tag{8}$$

where Δf corresponds to the trellis tilt introduced in (4).

As considered in [19], the receiver model contains a complex bandpass filter with the pass band at the low-IF. As a consequence of the impulse response of the bandpass filter $g_{\mathrm{IF,cmplx}}(\tau)$, which has a length of T_g, the memory of the entire system increases by L_g symbols where $(L_g - 1) \cdot T_{\mathrm{s}} < T_g \le L_g \cdot T_{\mathrm{s}}$ holds. The received signal is given by the convolution of the complex IF signal distorted by additive white Gaussian noise $n(t)$[1] and the complex bandpass filter

$$z(t) = \int_{-\infty}^{\infty}\left(\sqrt{\frac{E_{\mathrm{s}}}{T_{\mathrm{s}}}}e^{j\psi_{\mathrm{IF}}(\tau)} + n(\tau)\right) g_{\mathrm{IF,cmplx}}(t - \tau)d\tau, \tag{9}$$

which is sampled with rate $\frac{M}{T_{\mathrm{s}}}$ and quantized with 1-bit resolution in the in-phase component and the quadrature-phase component, where M is the oversampling factor with respect to the transmit symbol duration T_{s}. The corresponding system model, based on the conventional input alphabet α_k and low IF, is illustrated in Fig. 2. The equivalent notation based on the input alphabet x_k is used in the following.

3) Discrete-Time Modeling: The discrete time model, illustrated in Fig. 3, is described in the following. Rewriting the phase expression in (7) using (5) with a vector notation gives

$$\begin{aligned}\boldsymbol{\psi}_{\mathrm{IF},k}(\tilde{s}_k, n_{\mathrm{IF}}) =& \boldsymbol{\psi}_{\mathrm{IF},k}\left(\left[\beta_{k-L_{\mathrm{cpm}}}, x_{k-L_{\mathrm{cpm}}+1}^{k}\right], n_{\mathrm{IF}}\right) \\ =& \left(2\pi\frac{\beta_{k-L_{\mathrm{cpm}}} + 1}{P_{\mathrm{cpm}}}\right. \\ &\left. + \pi h(M_{\mathrm{cpm}} - 1)\left(L_{\mathrm{cpm}} - 1\right) + \varphi_0\right) \cdot \mathbf{1}_{MD} \\ &+ \pi\left(2n_{\mathrm{IF}} + h(M_{\mathrm{cpm}} - 1)\right)\frac{[1, \ldots, MD]^T}{MD} \\ &+ 4\pi h \boldsymbol{F}\boldsymbol{U} x_{k-L_{\mathrm{cpm}}+1}^{k} \\ &- 2\pi h(M_{\mathrm{cpm}} - 1)\boldsymbol{F}\boldsymbol{U}\mathbf{1}_{L_{\mathrm{cpm}}},\end{aligned} \tag{10}$$

where $\mathbf{1}_i$ is a column vector filled with ones of length i. The description with a D fold higher sampling rate allows us to model the aliasing effects which can possibly occur with receive filters having a larger bandwidth as can be described

[1]The statistics of a white noise process are invariant with respect to frequency transformations.

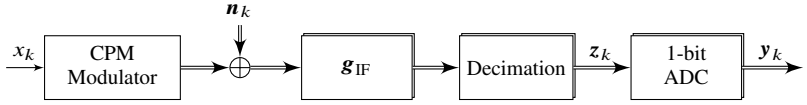

Fig. 3. Discrete-time representation of the effective system model, Markov source model, 1-bit quantization and oversampling at the receiver

with the sampling rate of the receiver $\frac{M}{T_\mathrm{s}}$. The matrix multiplication with matrix $\boldsymbol{F}$ expresses the convolution with the phase response function and its corresponding time inversion. The filter matrix $\boldsymbol{F}$ of dimensions $MD \times MD(L_\mathrm{cpm}+1)-1$ is given by

$$\boldsymbol{F} = \begin{pmatrix} \left[\ \boldsymbol{f}_\mathrm{r}^T\ \right] & 0 \cdots & 0 \\ \frac{1}{2}\ \left[\ \boldsymbol{f}_\mathrm{r}^T\ \right] & 0 \cdots 0 & \\ \ddots & \ddots & \ddots \\ \frac{1}{2} \cdots & \frac{1}{2}\ \left[\ \boldsymbol{f}_\mathrm{r}^T\ \right] & \end{pmatrix}, \tag{11}$$

where $\boldsymbol{f}_\mathrm{r} = [f(L_\mathrm{cpm}T_\mathrm{s}), f(\frac{L_\mathrm{cpm}MD-1}{MD}T_\mathrm{s}), \ldots, f(\frac{T_\mathrm{s}}{MD}))]^T$ with length MDL_cpm is the reversely sampled frequency response function in the interval $0 < \tau \leq L_\mathrm{cpm}T_\mathrm{s}$.

The upsampling matrix $\boldsymbol{U}$ with dimensions $(L_\mathrm{cpm}+1)MD - 1 \times L_\mathrm{cpm}$ is given by

$$U_{i,j} = \begin{cases} 1 & \text{for } i = jMD, \\ 0 & \text{otherwise}, \end{cases} \tag{12}$$

where i and j are positive integers accounting for the row and the column, respectively.

Because CPM signals are not strictly bandlimited, we consider a receive filter without strict bandlimitation. In order to model the corresponding aliasing effect appropriately the noise filtering and the waveform are described on a sampling grid which has an 8 times higher resolution than the sampling resolution at the receiver, i.e., $D = 8$, followed by a decimation.

Finally, the complex waveform is filtered and quantized in the passband such that the received signal is given by

$$\boldsymbol{y}_{k-N}^k = Q\left(\boldsymbol{z}_{k-N}^k\right) \tag{13}$$

$$= Q\left(\boldsymbol{D}\ \boldsymbol{G}_\mathrm{IF}\left[\sqrt{\frac{E_\mathrm{s}}{T_\mathrm{s}}}e^{\boldsymbol{\psi}_{\mathrm{IF},k-L_g-N}^k} + \boldsymbol{n}_{k-L_g-N}^k\right]\right). \tag{14}$$

The quantization is described by $y_{k,m} = Q(z_{k,m})$, where $Q(z_{k,m}) = \mathrm{sgn}(\mathrm{Re}\left\{z_{k,m}\right\}) + j\mathrm{sgn}(\mathrm{Im}\left\{z_{k,m}\right\})$, such that $y_{k,m} \in \{1+j, 1-j, -1+j, -1-j\}$. The quantization operator applies element-wise with $Q\{\boldsymbol{z}_k\} = [Q(z_{k,1}), \ldots, Q(z_{k,M})]^T$. $\boldsymbol{G}_\mathrm{IF}$ represents the filter matrix of the receive filter $g_{\mathrm{IF,cmplx}}(t)$, $\boldsymbol{n}_{k-L_g-N}^k$ is a vector containing complex zero-mean white Gaussian noise samples with variance $\sigma_n^2 = N_0$ and $\boldsymbol{D}$ denotes the decimation matrix. The decimation matrix $\boldsymbol{D}$ of dimensions $M(N+1) \times MD(N+1)$ is given by

$$D_{i,j} = \begin{cases} 1 & \text{for } j = (i-1)D+1, \\ 0 & \text{otherwise}. \end{cases} \tag{15}$$

The structure of the filter matrix of dimensions $MD(N+1) \times MD(L_g+N+1)$ is given by

$$\boldsymbol{G}_\mathrm{IF}(\cdot) = \frac{1}{\left\|\boldsymbol{g}_\mathrm{r,IF}\right\|_2}\begin{pmatrix} \left[\ \boldsymbol{g}_\mathrm{r,IF}^T\ \right] & 0 \cdots & 0 & 0 \\ 0\ \left[\ \boldsymbol{g}_\mathrm{r,IF}^T\ \right] & 0 \cdots 0 & 0 & \\ \ddots & \ddots & \ddots & \\ 0 \cdots & 0\ \left[\ \boldsymbol{g}_\mathrm{r,IF}^T\ \right] & 0 & \end{pmatrix}, \tag{16}$$

where $\boldsymbol{g}_\mathrm{r,IF} = [g_{\mathrm{IF,cmplx}}(L_gT_\mathrm{s}), g_{\mathrm{IF,cmplx}}(\frac{T_\mathrm{s}}{MD}(L_gMD - 1)), \ldots, g_{\mathrm{IF,cmplx}}(\frac{T_\mathrm{s}}{MD})]^T$ which is filled with zeros for receive filters with shorter impulse response. With this, the effective system model which is finally considered for computation of the rate based on the transmit symbols x_k is illustrated in Fig. 3. The CPM modulator in Fig. 3 transforms the input sequence x^n into the transmit signal $\sqrt{\frac{E_\mathrm{s}}{T_\mathrm{s}}}e^{j\boldsymbol{\psi}_{\mathrm{IF},k}(\tilde{s}_k, n_\mathrm{IF})}$, where $\boldsymbol{\psi}_{\mathrm{IF},k}(\tilde{s}_k, n_\mathrm{IF})$ is described with (10).

III. The Achievable Rate

The achievable rate for channels with memory can be computed by making advantage of the Shannon-McMillan-Breiman theorem as proposed in [20], [21]. In order to reduce the complexity of the computation of the achievable rate a simplifying auxiliary channel law is used, which corresponds to a lower bound on the achievable rate.

A. Lower Bound on the Achievable Rate using an Auxiliary Channel Law

As stated in [21] the achievable rate is lower-bounded by

$$\lim_{n\to\infty}\frac{1}{n}I(X^n;\boldsymbol{Y}^n) \geq \lim_{n\to\infty}\frac{1}{n}(-\log_2 W(\boldsymbol{y}^n) + \log_2 W(\boldsymbol{y}^n|x^n)), \tag{17}$$

where the RHS can be practically evaluated with a long sequence of channel output observations of the actual channel $\boldsymbol{y}^n$, i.e., following $P(\boldsymbol{y}_k|\boldsymbol{y}^{k-1}, x^n)$. The quantities $W(\cdot)$ and $W(\cdot|\cdot)$ on the RHS of (17) are probabilities according to an auxiliary channel law $W(\boldsymbol{y}_k|\boldsymbol{y}^{k-1}, x^n)$. For the computation the BCJR forward recursion is applied as described in detail for a channel with oversampling at the receiver, i.e., in [22].

B. The Auxiliary Channel Law

The auxiliary channel law shall provide an adequate statistical description of the channel output of the actual channel $P(\boldsymbol{y}_k|\boldsymbol{y}^{k-1}, x^n)$ such that

$$P(\boldsymbol{y}_k|\boldsymbol{y}^{k-1}, x^n) \approx W(\boldsymbol{y}_k|\boldsymbol{y}^{k-1}, x^n). \tag{18}$$

The auxiliary channel law takes into account N previous channel realizations, $L_{\mathrm{cpm}} + L_{\mathrm{g}} + N - 1$ previous transmit symbols and the absolute phase state, and is given by

$$\begin{aligned} W(\boldsymbol{y}_k|\boldsymbol{y}^{k-1}, x^n) &= P(\boldsymbol{y}_k|\boldsymbol{y}_{k-N}^{k-1}, x^n) \\ &= P(\boldsymbol{y}_k|\boldsymbol{y}_{k-N}^{k-1}, \beta_{k-L_{\mathrm{cpm}}-L_g-N}, x_{k-L_{\mathrm{cpm}}-L_{\mathrm{g}}-N+1}^{k}) \\ &= P(\boldsymbol{y}_k|\boldsymbol{y}_{k-N}^{k-1}, \beta_{k-L}, x_{k-L+1}^{k}) = \frac{P(\boldsymbol{y}_{k-N}^{k}|\beta_{k-L}, x_{k-L+1}^{k})}{P(\boldsymbol{y}_{k-N}^{k-1}|\beta_{k-L}, x_{k-L+1}^{k-1})}, \end{aligned} \tag{19}$$

with $L = L_{\mathrm{cpm}} + L_g + N$. With this, the auxiliary channel law ignores the potential dependency on further previous channel realizations, which exists due to the correlation of the noise samples arising from receive filters with long impulse responses. Taking into account the receive filter and its impact on the noise correlation and the waveform implies the need for an extended state representation termed s_k instead of $\tilde{s}_k$. To be more detailed, the channel states are case sensitive. In this regard, when writing the auxiliary channel law based on a state notation $P(\boldsymbol{y}_k|\boldsymbol{y}_{k-N}^{k-1}, s_{k-1}, s_k)$ the following cases are distinguished:

$$s_k = \begin{cases} [\beta_{k-L+1}, x_{k-L+2}^{k}], & \text{if } L > 1, \\ [\beta_k], & \text{if } L = 1, \end{cases}$$

where β_{k-L+1} is not named in (19) because it can be described by β_{k-L} and x_{k-L+1}.

In this regard, the conditional probability density function of the unquantized received signal, cf. (14), is described by

$$\begin{aligned} p(\boldsymbol{z}_{k-N}^{k}|s_k, s_{k-1}) &= \frac{1}{\sqrt{(2\pi)^{2M(N+1)}\,|\boldsymbol{R}|}} \\ &\times \exp\left(-\frac{1}{2}\left([\boldsymbol{z}_{k-N}^{k}]' - \boldsymbol{\mu}_x\right)^T \boldsymbol{R}^{-1}\left([\boldsymbol{z}_{k-N}^{k}]' - \boldsymbol{\mu}_x\right)\right), \end{aligned} \tag{20}$$

where $|\cdot|$ denotes the determinant, $[\boldsymbol{z}_{k-N}^{k}]' = \left[\mathrm{Re}\left\{\boldsymbol{z}_{k-N}^{k}\right\}^T, \mathrm{Im}\left\{\boldsymbol{z}_{k-N}^{k}\right\}^T\right]^T$ and the mean vector $\boldsymbol{\mu}_x$ contains the real and imaginary components in a stacked fashion as given by

$$\boldsymbol{\mu}_x = \begin{bmatrix} \boldsymbol{\mu}_{\mathrm{Re}} \\ \boldsymbol{\mu}_{\mathrm{Im}} \end{bmatrix} = \begin{bmatrix} \mathrm{Re}\left\{\boldsymbol{D}\ \boldsymbol{G}_{\mathrm{IF}}\left[\sqrt{\frac{E_{\mathrm{s}}}{T_{\mathrm{s}}}} e^{\boldsymbol{\psi}_{\mathrm{IF},k-L_g-N}^{k}}\right]\right\} \\ \mathrm{Im}\left\{\boldsymbol{D}\ \boldsymbol{G}_{\mathrm{IF}}\left[\sqrt{\frac{E_{\mathrm{s}}}{T_{\mathrm{s}}}} e^{\boldsymbol{\psi}_{\mathrm{IF},k-L_g-N}^{k}}\right]\right\} \end{bmatrix}. \tag{21}$$

With this, the covariance matrix is denoted as

$$\begin{aligned} \boldsymbol{R} = \mathrm{E}\Bigg\{ &\begin{bmatrix} \boldsymbol{D}\ \mathrm{Re}\{\boldsymbol{G}_{\mathrm{IF}}\} & -\boldsymbol{D}\ \mathrm{Im}\{\boldsymbol{G}_{\mathrm{IF}}\} \\ \boldsymbol{D}\ \mathrm{Im}\{\boldsymbol{G}_{\mathrm{IF}}\} & \boldsymbol{D}\ \mathrm{Re}\{\boldsymbol{G}_{\mathrm{IF}}\} \end{bmatrix} \begin{bmatrix} \mathrm{Re}\left\{\boldsymbol{n}_{k-L_g-N}^{k}\right\} \\ \mathrm{Im}\left\{\boldsymbol{n}_{k-L_g-N}^{k}\right\} \end{bmatrix} \\ &\times \begin{bmatrix} \mathrm{Re}\left\{\boldsymbol{n}_{k-L_g-N}^{k}\right\} \\ \mathrm{Im}\left\{\boldsymbol{n}_{k-L_g-N}^{k}\right\} \end{bmatrix}^T \begin{bmatrix} \boldsymbol{D}\ \mathrm{Re}\{\boldsymbol{G}_{\mathrm{IF}}\} & -\boldsymbol{D}\ \mathrm{Im}\{\boldsymbol{G}_{\mathrm{IF}}\} \\ \boldsymbol{D}\ \mathrm{Im}\{\boldsymbol{G}_{\mathrm{IF}}\} & \boldsymbol{D}\ \mathrm{Re}\{\boldsymbol{G}_{\mathrm{IF}}\} \end{bmatrix}^T \Bigg\}. \end{aligned} \tag{22}$$

By integration over the quantization interval the channel output probabilities are obtained as

$$P(\boldsymbol{y}_{k-N}^{k}|s_k, s_{k-1}) = \int\limits_{\boldsymbol{z}_{k-N}^{k} \in \mathbb{Y}_{k-N}^{k}} p(\boldsymbol{z}_{k-N}^{k-1}|s_k, s_{k-1}) d\boldsymbol{z}_{k-N}^{k}, \tag{23}$$

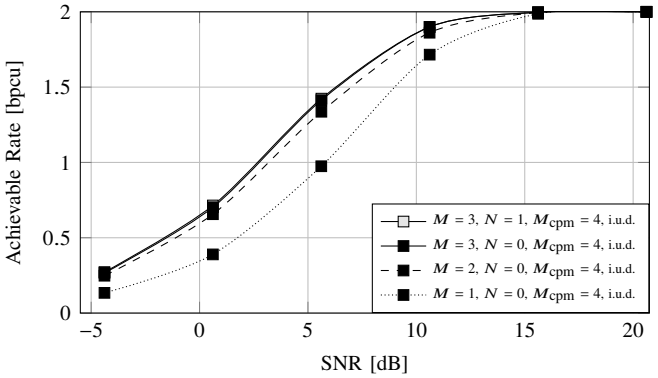

Fig. 4. Effect of the oversampling factor M on the achievable rate, $n_{\mathrm{IF}} = 0$; the curves for $M = 3$ with $N = 1$ and $N = 0$ superpose each other in part

where $\mathbb{Y}_{k-N}^{k}$ represents the quantization interval which belongs to the channel output symbol $\boldsymbol{y}_{k-N}^{k}$, cf. (14).

IV. Numerical Results

Standard constellations are considered with $M_{\mathrm{cpm}} = 4, 8$ and 16 with the modulation index $h = \frac{1}{M_{\mathrm{cpm}}}$. The considered frequency pulse is given by $g_f(\tau) = \frac{1}{2 \cdot T_{\mathrm{s}}} \mathrm{rect}\left(\frac{\tau - T_{\mathrm{s}}/2}{T_{\mathrm{s}}}\right)$.

In order to widely preserve the transmit waveform and especially its zero-crossings a suboptimal noise filtering in terms of a bandpass filter with relatively large bandwidth is considered, i.e.,

$$g_{\mathrm{IF}}(t) = \sqrt{\frac{1}{T_g}} \mathrm{rect}\left(\frac{t - T_{\mathrm{s}}/2}{T_g}\right) \cdot e^{j2\pi\left(\Delta f + \frac{n_{\mathrm{IF}}}{T_{\mathrm{s}}}\right)(t - T_{\mathrm{s}}/2)}, \tag{24}$$

where $T_g = \frac{1}{2} \cdot T_{\mathrm{s}}$.[2] With this, the noise samples are not correlated for $M \leq 2$. As a consequence the auxiliary channel model can be chosen with $N = 0$ without approximation, i.e., the auxiliary channel is equivalent to the actual channel. For $M = 3$ noise correlation is involved in the auxiliary channel law $W(\cdot)$ with $N = 0$ such that the samples within one received oversampling block $\boldsymbol{y}_k$ are correlated, but there is no correlation between different blocks. Note that by the choice $N = 0$ the correlation between subsequent channel output blocks $\boldsymbol{y}_{k-1}$, $\boldsymbol{y}_k$ is ignored, which would be taken into account with $N = 1$.

The SNR is given by the ratio between the transmit power and the product of the noise power spectral density N_0 and the two-sided 90% power containment bandwidth $B_{90\%}$

$$\mathrm{SNR} = \frac{\lim_{T \to \infty} \frac{1}{T} \int_T |x(t)|^2 \, dt}{N_0 \ B_{90\%}}. \tag{25}$$

Note that the discrete noise samples in (14) have a variance of $\sigma_n^2 = N_0$. Considering that 5% out of band radiation can be tolerated at the lower and higher frequencies we get

$$\int_{-\infty}^{B_{90\%,\uparrow}} S(f) df = \int_{B_{90\%,\downarrow}}^{\infty} S(f) df = 0.95 \int_{-\infty}^{\infty} S(f) df, \tag{26}$$

[2]Because the CPM signal has infinite bandwidth any receive filter causes a change of the waveform to some extent.

where $S(f)$ denotes the power spectral density of the complex baseband representation at zero-IF $x(t) = \sqrt{\frac{E_s}{T_s}} e^{j\phi(t)}$. With this, the power containment bandwidth is given by $B_{90\%} = B_{90\%,\uparrow} - B_{90\%,\downarrow}$. A number of methods for the computation of the spectrum for CPM signals exist, e.g., [23]. Here, the power spectral density is estimated based on the sample autocorrelation function of one transmit signal that spans over a sequence of 10^6 symbols. For computing the sample autocorrelation function we consider an 8-fold higher sampling grid ($D = 8$) as compared to the sampling rate at the receiver.

A. Oversampling

In Fig. 4 it is shown how oversampling increases the achievable rate by providing additional information about the symbol transitions which convey the information. For the beginning we consider a conventional setup with $M_{\text{cpm}} = 4$ and $n_{\text{IF}} = 0$. The significant benefit of oversampling is due to the fact that the quantizer output only provides hard decisions when sampling at symbol rate. With $N = 1$ a dependency on the previous channel realization $\boldsymbol{y}_{k-1}$ is taken into account in the channel law when sampling with 3-fold oversampling rate. Due to the fact that the considered impulse response of the receive filter is relatively short, there is only a marginal benefit when exploiting this dependency. Hence, the following results rely on the auxiliary channel model with $N = 0$.

B. Higher Modulation Order

Especially at high SNR the additional degrees of freedom at the receiver can be exploited by considering a higher modulation order. In this regard, it is shown in Fig. 5 that considering $M_{\text{cpm}} = 8, 16$ significantly increases the achievable rate. However, the benefit of $M_{\text{cpm}} = 16$ in comparison to $M_{\text{cpm}} = 8$ in terms of achievable rate is only marginal and in some cases the performance is even worse. Here a tailored sequence design might further increases the achievable rate. Fig. 5 also shows that the choice of the intermediate frequency has only an marginal effect on the achievable rate.

C. Effective Oversampling Ratio

Using the power spectral density the 90% power containment bandwidth is extracted and utilized for computation of the spectral efficiency. The spectral efficiency referring to the 90% power containment bandwidth is given by

$$\text{spectral eff.} = \frac{I_{\text{bpcu}}}{T_{\text{s}} B_{90\%}} \text{ [bit/s/Hz]}, \tag{27}$$

where I_{bpcu} is the achievable rate w.r.t. one symbol duration T_{s}. For a comprehensive comparison the effective oversampling ratio needs to be evaluated. The oversampling ratio referring to the 90% power containment bandwidth is given by

$$\text{OSR}' = M \left(B_{90\%} \cdot T_{\text{s}}\right)^{-1}. \tag{28}$$

The spectral efficiency for the high SNR limit is illustrated in Fig. 6 together with the corresponding effective oversampling ratio OSR′. The results have been compared with approaches from the literature and especially with recent results from

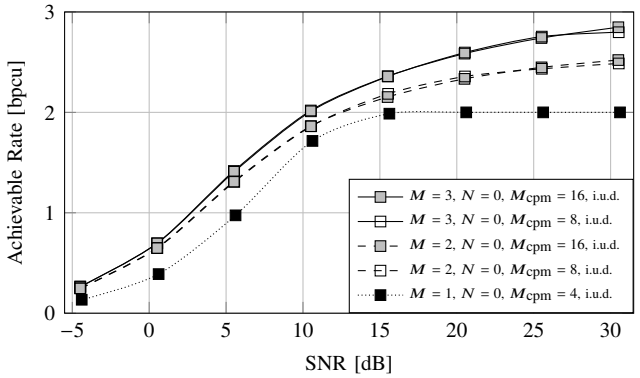

(a) $n_{\text{IF}} = 0$

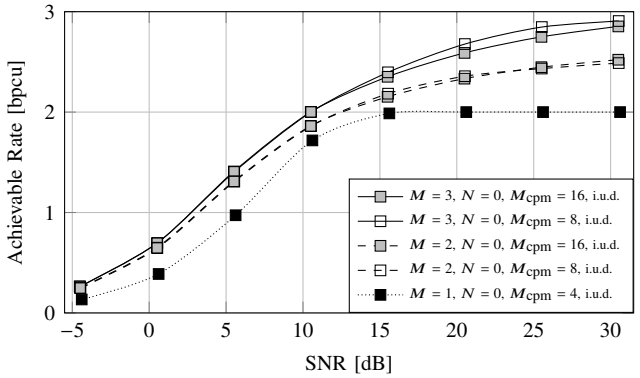

(b) $n_{\text{IF}} = 1$

Fig. 5. Effect of the modulation order on the achievable rate

a related study with root raised cosine (RRC) filtering and sequence design [9]. The proposed communication methods shows a lower performance compared to [9] in terms of spectral efficiency w.r.t. the given power containment bandwidth criterion. However, unlike the approach in [9], the proposed CPM signals have a constant envelope, such that energy efficient transmitters can be employed. The proposed approaches are also compared with a flash-ADC based scheme where the ADC uses the same number of comparator operations per time interval. The spectral efficiency of the flash-ADC based scheme is calculated w.r.t. $B_{90\%}$ where we have assumed a flat spectrum. Also the spectral efficiency for the Zakai bandlimited processes over the noiseless channel [5] is illustrated, which is not normalized w.r.t. $B_{90\%}$because it has no spectral representation.

V. Conclusions

The achievable rate of a system with continuous phase modulation, 1-bit quantization and oversampling at the receiver has been studied. It turns out that oversampling is beneficial in all considered cases because the additional samples implicitly provide information on phase transitions which convey the information. When higher order modulations are considered oversampling is beneficial in terms of achievable rate also in the high SNR regime. The spectral efficiency together with the effective oversampling ratio show a slightly lower

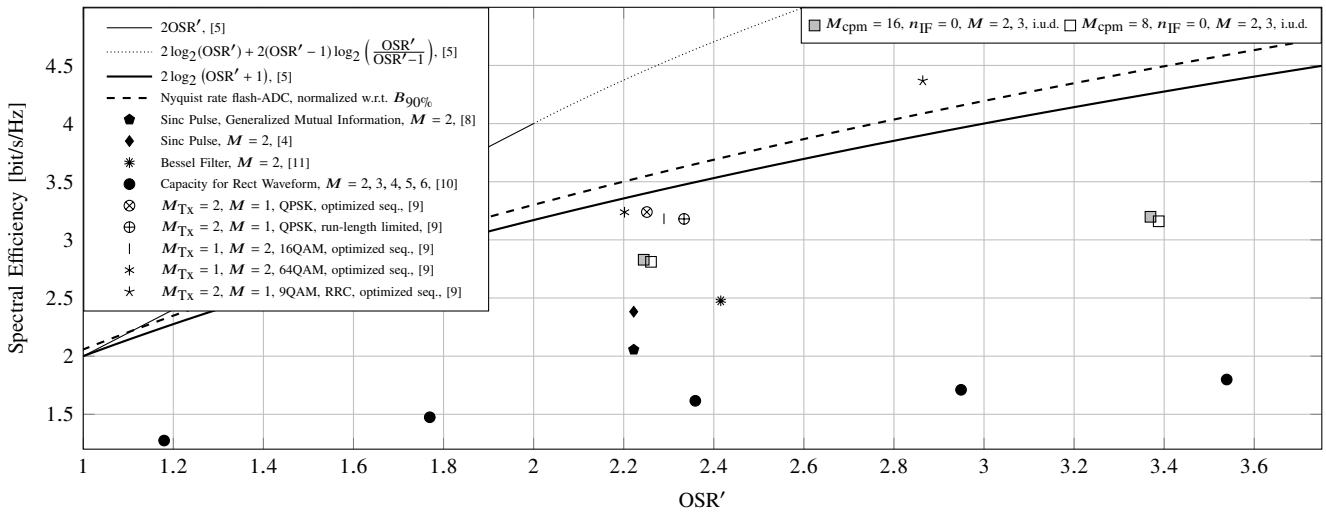

Fig. 6. Spectral efficiency in relation to the effective oversampling ratio in the high SNR limit

performance than some methods known from the literature on noisy channels with 1-bit quantization and oversampling at the receiver. Nevertheless, different to the existing methods the proposed system implies signals with constant envelope which is favorable for the utilization of energy-efficient power amplifiers at the transmitter.

ACKNOWLEDGMENT

This work has been supported in part by the German Research Foundation (DFG) within the SFB 912 "Highly Adaptive Energy-Efficient Computing (HAEC)".

REFERENCES

[1] J. Anderson, T. Aulin, and C. E. Sundberg, *Digital Phase Modulation*. New York: Plenum Press, 1986.

[2] C. E. Sundberg, "Continuous phase modulation," *IEEE Commun. Mag.*, vol. 24, no. 4, pp. 25–38, April 1986.

[3] M. H. M. Costa, "A practical demodulator for continuous phase modulation," in *Proc. IEEE Int. Symp. Inform. Theory (ISIT)*, Trondheim, Norway, Jun 1994, p. 88.

[4] E. N. Gilbert, "Increased information rate by oversampling," *IEEE Trans. Inf. Theory*, vol. 39, no. 6, pp. 1973–1976, Nov. 1993.

[5] S. Shamai (Shitz), "Information rates by oversampling the sign of a bandlimited process," *IEEE Trans. Inf. Theory*, vol. 40, no. 4, pp. 1230–1236, Jul. 1994.

[6] M. Zakai, "Band-limited functions and the sampling theorem," *Information and Control*, vol. 8, no. 2, pp. 143 – 158, 1965.

[7] T. Koch and A. Lapidoth, "Increased capacity per unit-cost by oversampling," in *Proc. of the IEEE Convention of Electrical and Electronics Engineers in Israel*, Eilat, Israel, Nov. 2010.

[8] W. Zhang, "A general framework for transmission with transceiver distortion and some applications," *IEEE Trans. Commun.*, vol. 60, no. 2, pp. 384–399, Feb. 2012.

[9] L. Landau, M. Dörpinghaus, and G. P. Fettweis, "1-bit quantization and oversampling at the receiver: Communication over bandlimited channels with noise," *IEEE Commun. Lett.*, vol. 21, no. 5, pp. 1007–1010, May 2017.

[10] S. Krone and G. P. Fettweis, "Capacity of communications channels with 1-bit quantization and oversampling at the receiver," in *Proc. of the IEEE Sarnoff Symp.*, Newark, New Jersey, USA, May 2012.

[11] ——, "Communications with 1-bit quantization and oversampling at the receiver: Benefiting from inter-symbol-interference," in *Proc. of the IEEE Int. Symposium on Personal, Indoor, and Mobile Radio Communications*, Sydney, Australia, Sep. 2012.

[12] L. Landau and G. P. Fettweis, "On reconstructable ASK-sequences for receivers employing 1-bit quantization and oversampling," in *Proc. of the IEEE Int. Conf. on Ultra-Wideband*, Paris, France, Sep. 2014.

[13] L. Landau, M. Dörpinghaus, and G. P. Fettweis, "Communications employing 1-bit quantization and oversampling at the receiver: Faster-than-Nyquist signaling and sequence design," in *Proc. of the IEEE Int. Conf. on Ubiquitous Wireless Broadband*, Montreal, Canada, Oct. 2015.

[14] S. Bender, L. Landau, M. Dörpinghaus, and G. P. Fettweis, "Communication with 1-bit quantization and oversampling at the receiver: Spectral constrained waveform optimization," in *Proc. of the IEEE Int. Workshop on Signal Processing Advances in Wireless Communications*, Edinburgh, UK, Jul. 2016.

[15] L. Landau, S. Krone, and G. P. Fettweis, "Intersymbol-interference design for maximum information rates with 1-bit quantization and oversampling at the receiver," in *Proc. of the International ITG Conference on Systems, Communications and Coding*, Munich, Germany, Jan. 2013.

[16] A. Gokceoglu, E. Björnson, E. G. Larsson, and M. Valkama, "Waveform design for massive MISO downlink with energy-efficient receivers adopting 1-bit ADCs," in *Proc. IEEE Int. Conf. Commun. (ICC)*, Kuala Lumpur, Malaysia, May 2016, pp. 1–7.

[17] ——, "Spatio-temporal waveform design for multi-user massive MIMO downlink with 1-bit receivers," *IEEE J. Sel. Topics Signal Process.*, Nov. 2016.

[18] B. E. Rimoldi, "A decomposition approach to CPM," *IEEE Trans. Inf. Theory*, vol. 34, no. 2, pp. 260–270, Mar. 1988.

[19] T. Scholand and P. Jung, "Intermediate frequency zero-crossing detection of filtered MSK based on irregular sampling," *European Trans. on Telecommunications*, vol. 18, no. 7, pp. 669–683, 2007.

[20] H. D. Pfister, J. B. Soriaga, and P. H. Siegel, "On the achievable information rates of finite state ISI channels," in *Proc. IEEE Glob. Comm. Conf. (GLOBECOM)*, San Antonio, TX, USA, Nov. 2001.

[21] D. M. Arnold, H.-A. Loeliger, P. O. Vontobel, A. Kavcic, and W. Zeng, "Simulation-based computation of information rates for channels with memory," *IEEE Trans. Inf. Theory*, vol. 52, no. 8, pp. 3498–3508, Aug. 2006.

[22] L. Landau and G. P. Fettweis, "Information rates employing 1-bit quantization and oversampling," in *Proc. of the IEEE Int. Workshop on Signal Processing Advances in Wireless Communications*, Toronto, Canada, Jun. 2014.

[23] R. R. Anderson and J. Salz, "Spectra of digital FM," *Bell System Technical Journal*, vol. 44, no. 6, pp. 1165–1189, 1965.